Jurnal Kejuruteraan 35(6) 2023: 1403-1417
https://doi.org/10.17576/jkukm-2023-35(6)-13

# The Effect of Graphene, Silica, And Natural Dust Particles On The Performances of Multiple Types Of Solar Photovoltaic Modules

Israa Amer Dahham[a], Muhammad Ammirul Atiqi Mohd Zainuri [a,b*], Ali Abdulabbas Abdullah[c], Mohd Faizal Fauzan[b] & Qais Hamid Jeflawe[d]

[a] *Department of Electrical, Electronic and System Engineering, Faculty of Engineering and Built Environment, Universiti Kebangsaan Malaysia, 43600, Bangi Selangor, Malaysia*

[b] *Solar Energy Researcy Institute, Universiti Kebangsaan Malaysia, 43600, Bangi Selangor, Malaysia*

[c] *Technical College Almusaib, Al-Furat Al-Ausat Technical University*

[d] *Ministry of Electricity, Iraq*

**Corresponding author: ammirrulatiqi@ukm.edu.my*

*Received 13February 2023, Received in revised form 9 May 2023*
*Accepted 9 June 2023, Available online 30 November 2023*

ABSTRACT

*Desertification and industrial pollution environment can significantly degrade photovoltaic cells performance. Accumulated dust on the surface of a photovoltaic module can partially hinder incident light and consequently degrade optical to electrical energy conversion. Dust properties play a major role in deteriorating solar system performance. Thus, this paper presents extensive investigations on the UV- absorbance, light transmittance and reflectance through an accumulated dust layer. Dust characterization; focusing on its spectral and crystallographic properties of three types of dust (Graphene, Silica, and natural), was carried out to evaluate the degradation rate of the output power for three types of solar PV modules (monocrystalline, polycrystalline, and thin-film). Spectrophotometric analysis was conducted to determine UV light absorbance and light transmittance through the three types of dust. X-Ray Diffraction (XRD) and Scanning Electron Microscopy (SEM) tests were conducted to evaluate the effect of dust crystallinity on light reflectance. A lab-scale setup was used to examine the performances of the three solar PV modules under clean and polluted conditions. Results indicated that Graphene dust exhibits severe UV light absorbance, and its crystalline form increases light reflectance from the surfaces of the modules. However, Silica and natural dust showed a little UV absorbance. Among the three types of the solar PV modules, thin-film panel showed the highest degradation under polluted conditions as compared to the other modules. Therefore, thin film solar module is not recommended for areas with high density of dust.*

*Keywords: Photovoltaic system; dust effect on PV cell; dust characteristics; dust deposition rate*

## INTRODUCTION

Recently, solar energy utilization through photovoltaic (PV) technology has been widely expanding. PV cells directly convert sunlight energy into electricity with ever decreasing in manufacturing costs (Chanchangi et al. 2020). However, the accumulation of dust on the surface of a PV module negatively impacts its output power (Costa et al. 2018). The effect of dust on the PV performance depends on many factors; dust mass density accumulated on the PV module surface, dust particle size, and dust characteristics (Hussain et al. 2017; Fountoukis et al. 2018). Extensive performance analysis of PV modules under dust accumulation conditions were performed (Darwish 2013). The effect of the physical and chemical properties of the dust on the PV module performance was backdated to 1993 (El-Shobokshy and Hussain 1993). An indoor laboratory study showed that 30-40% reduction in output power of PV modules was observed due to six different types of dust spread on their surfaces (Kazem and Chichan 2019).

Alnasser et al. (2020) sprayed 100 g/m2 of sand, cement, and gypsum powders on PV modules to investigate the PV performance degradation under opaque layer of dust. The results showed that 12%, 14%, and 9% output power drop were noticed for the sand, cement, and gypsum powders respectively. Chen et al. (2020) observed two main types of dust in east of China ($SiO_2$ and $CaCO_3$) that accumulate up to 0.664 g/m2 resulting in 7.4% reduction in PV output power.

Recent investigations in four Iraqi districts (Baghdad, Najaf, Karbala, and Fao) were performed to evaluate the effect of both natural and urban-based dusts on solar systems performance. The study demonstrated a time-dependent and a non-linear degradation in the output power of the PV modules (Chaichan et al. 2020). Average degradation rate for PV modules was reported by Saidan et al. (2016) to be 6.24% for a daily dust deposition, 11.8% per one week, and 18.74% for one month in Baghdad city. The degradations were reported to be a dust-type dependent indicating the necessity to study the effect of the desert-based and urban-based dusts on the PV modules (Hassan et al. 2017). Many researchers have committed to investigate the effect of dust composition and characteristics on the PV module performance (Styszko et al. 2017; Fujiwara et al. 2011; Bi et al. 2013; Sarver et al. 2013). The source of the urban-based dust is industry and fuel combustion for transportation and electricity generation (Benatiallah et al. 2012; Pang et al. 2006). Urban-based dust is consisted of fine particles (less than 50 μm) and shows greater adhesion to the surfaces of PV modules (El-Shobokshy and Hussain 1993; Hinds 1999). It was concluded that carbon particles can reduce the power output of the PV module by 90% when the deposition density of the carbon dust was 25 gm/m2. Natural dust is a soil-sourced and its characteristics vary from region to region. Sulaiman et al. (2011), Khatib et al. (2013), and John et al. (2016) studied many types of natural dusts and found that limestone, Calcium carbonate, Silica, Sand, and Red Soil had major deterioration effects on the power output of the PV modules due to their chemical, electrostatic, and charge distribution properties.

Comparison studies for different types of PV modules (monocrystalline and polycrystalline PV modules) under accumulated dust layer were researched by Ndiaye et al. (2013). Both monocrystalline and polycrystalline modules showed a power reduction of 17.75% and 18.02% respectively. Bashir et al. (2015) and Ali et al. (2016) investigated the effect of temperature on the performance of three types of PV modules (monocrystalline, polycrystalline, and single-junction amorphous silicon). They concluded that degradation rate increases with temperature increase and the single-junction amorphous silicon showed the highest performance ratio.

Literature shows that the performance of a PV module is a complex task. Most of the available information focuses on the effect of the dust mass density and dust particle size on the performance of the PV modules. Although XRD, XRF, and SEM tests were considered by Darwish et al. (2021) to investigate the effect of the dust morphology on the performance of the PV modules, but, to the best knowledge of the authors, dust morphology characteristics have less effect on the PV module performance than the dust spectral characteristics. Dust spectral characteristics determine the percent of the incident radiated energy absorbed by the dust particles resulting in a partial energy absorbance by the PV cells. Previous studies tried to relate chemical and physical characteristics of dusts with the degradation of PV modules Chanchangi et al. (2020), Kazem and Chaichan (2016), Kasmerski et al. (2016). However, to the best knowledge of the authors, none of the previous works has adequately performed spectrophotometric analysis to determine the capacity of dust particles to absorb incident radiation energy. Most of the previous work focused on the effect of opacity to hinder optical to electrical energy conversion. This work has managed to identify spectral conductive and spectral insulating dusts and their tendency to absorb incident radiation energy highlighting the novelty of this research. The previous researches extensively investigated the impact of dust properties (chemical and physical properties) on the rate of formation of dust layer on the surface of the PV modules. Li Yang and Irina Harun (2022) developed a framework for decision-makers to select a renewable energy option and to identify critical issues before implementing the selected option. The substantial conclusion of most of the previous research is related to the effect of the dust mass density (dust layer thickness) on the PV module performance. While the main conclusion of this research is related to the spectral conductivity of dust particles and their effectiveness in absorbing radiation energy.

This paper aims to investigate the effect of the spectral characteristics of Graphene, Silica, and natural dust on the performance of the PV cells. The study tried to measure the incident radiation absorbance and transmittance for the three types of dust within the Ultraviolet (UV), Visible (VIS), and Infrared (IR) spectra. It was observed that the high absorbance of incident radiation by the Graphene powder at the UV spectrum was independent of the thickness of the Graphene dust layer. While Silica and natural dust showed lower absorbance within the UV spectrum. The spectrally semi conductive materials (such as Graphene) have higher tendency for light absorbance than spectrally insulating materials (such as Silica and natural dust). The spectral semi conductive materials are easily excited when exposed to radiation and an atomic electron transition (jump) takes place leading to considerable absorbance of radiation energy. It was also found that Graphene disperses in neighbouring atmosphere and deposits as fine particulates on the surfaces of PV modules causing large absorbance of incident radiation regardless of its mass density. Therefore, the dispersion of the Graphene particles affects the site selection for PV modules installation. Air dispersion model based on the Gaussian-plume model was adopted in this study to predict the downwind and crosswind dispersion of the Graphene in neighbouring areas. Therefore, the novelty of this work is related to including the spectral characteristics of dust and dust dispersion domain in selecting sites for solar systems installation and construction. The site selection process for the solar system installation focuses on two main parameters: Conducting spectrophotometric analysis for the prevailing dusts in areas picked out for solar system installation to identify spectral semi conductive dusts. Therefore, mapping the dispersion and deposition of the semi conductive dust particles, is recommended to set dust dispersion boundaries of avoidance before the installation of PV modules.

## METHODOLOGY

### DISPERSION AND DEPOSITION MODEL

The dispersion of industrial dust particles depends on; emission rate, wind speed, plume rise, and atmospheric stability conditions [Macdonald, R., 2003]. Axial (downwind), horizontal (crosswind) and vertical dispersion of dust particles is promoted by advection and random wind perturbations. Graphene and carbon-based particles are considered the most adverse dust for PV modules. The rate of dispersion of the Graphene dust particles was calculated using Gaussian-plume model Macdonald (2003).

$$C_{(x,y,z)} = \frac{Q}{2\pi U\sigma_y\sigma_z}\exp(-\frac{y}{2\sigma_y^2})^2[\exp(-\frac{(z-H)^2}{2\sigma_z^2}) + \exp(-\frac{(z+H)^2}{2\sigma_z^2}] \qquad (1)$$

Where; $Q:$ source emissions rate of particulate (gm/s), $U:$ wind speed (m/s),
(gm/s), wind speed (m/s),
$\sigma_y:$ Crosswind dispersion coefficient (m), Vertical dispersion coefficient (m), $H:$effective stack height (m) = $H_s + \Delta H$ $H_s:$ stack height (m), $\Delta H:$ Plume rise (m)

$$\Delta H = \frac{21.425F^{0.75}}{U} \text{ for } F \le 55m^4/s^3 \qquad (2)$$

$$\Delta H = \frac{38.71F^{0.6}}{U} \text{ for } F \ge 55m^4/s^3 \qquad (3)$$

$$F = gV_sd^2(T_s - T_a)/4T_s \qquad (4)$$

Where; $F$: bouncy flux, $V_{s:}$ stack exit velocity (m/s), $d$: top inside stack diameter (m), $T_s$: stack gas temperature (K), $T_a$: ambient temperature (K), $g$: gravity (m/s2), $\sigma_y$ and $\sigma_z$ are strong functions of downwind distance (x) and atmospheric stability and can be determined from specific monographs or empirical equations.

The deposition rate is estimated using the following formulas Klassen et al. (1999):

$$F = gV_sd^2(T_s - T_a)/4T_s \qquad (5)$$

$$F = gV_sd^2(T_s - T_a)/4T_s \qquad (6)$$

Where; $N:$deposition rate (gm/m$^2$s), $U:$wind velocity (m/s), $C_\alpha:$ Graphene concentration (gm/m$^3$), $\eta:$impact efficiency of PV surface, $D_t:$PV module thickness (m), $U_i:$Particle velocity (m/s), $S:$Graphene particle diameter (m), $F:$ unit flux of air arriving per unit area at 1 m/s = 1

The deposit rate of the Graphene particles on the surface of the PV module was related to dispersion model and estimated using Microsoft Excel program. Then, the area of dispersion of the Graphene particles and the dust layer thickness on the surface of the PV module are calculated. To validate the model, a lab-scale setup was used to determine the effect of the Graphene, Silica, and natural dusts on the output power of three types of PV modules (monocrystalline, polycrystalline, and thin-film modules).

## MATERIALS AND LABORATORY TESTS

### SPECTROPHOTOMETRIC TESTS

Spectrophotometric measurements for Graphene, Silica, and natural dust were carried out using Holmarc UV/VIS/IR spectrophotometer with variable angle laser Ellipsometer. Standard glass sheets were first tested (no dust deposition) to measure their actual transmittance level. Then each type of dust was deposited in two different thickness layers.

Each sample was subjected to complete spectrum absorbance and transmittance tests. The absorbance and transmittance of each sample within the UV (Ultraviolet), VIS (Visible), and IR (Infrared) were measured to identify the degree of transmittance for each sample. Absorbance coefficient and energy gap for each sample were also determined to identify the semi conductivity of each dust. The absorbance coefficient is a measure of the attenuation of light intensity passing through the layer. The energy gap is a measure of energy required to promote a valence electron that attached to an atom.

## CRYSTALLOGRAPHIC ANALYSIS

Two imaging techniques (SEM and XRD) were used to study the morphology of deposited layers of three types of dust (Graphene, Silica, and natural dust). SEM is simply defined as a highly focused beam of electrons released from an electron gun and projected on a small spot of a sample. The sample emits high energy electron from its surface after being exposed to a focused beam of electrons. SEM tests were carried out using TESCAN VEGA III at the Nanotechnology and advanced material research center, University of Technology – Baghdad. XRD analysis was conducted to identify the crystallography of three types of dust (Graphene, Silica, and natural dust) using Shimadzu X-6000 diffract meter at the Nanotechnology and advanced material research center, University of Technology – Baghdad. The crystalline phases and the chemical compositions of the three types of dust were identified by means of X-Ray Diffract meter.

## PV PERFORMANCE MEASURING ARRANGEMENT

Three types of lab-scale solar panels (monocrystalline, polycrystalline, and thin-film panels) were used to investigate the effect of three types of dust on their performances. Table 1 demonstrates the characteristics of the three lab-scale solar panel.

TABLE 1. General Characteristics of lab-scale monocrystalline, polycrystalline, and thin-film PV modules

| No. | Characteristics | Monocrystalline Silicon panel | Polycrystalline Silicon panel | Thin-film crystalline silicon panel |
|---|---|---|---|---|
| 1 | Model | Copex Solar SFM-20 | Copex Solar SFPVP-20 | Copex Solar SWF-20W |
| 2 | Max Power (w) | 20 | 20 | 20 |
| 3 | Tolerance | ± 3% | ± 3% | ± 5% |
| 4 | Voltage (V) | 18 | 18 | 18.68 |
| 5 | Current (A) | 1.11 | 1.11 | 1.07 |
| 6 | Open circuit voltage (V) | 21.6 | 21.6 | 22.3 |
| 7 | Short circuit current (A) | 1.22 | 1.22 | 1.13 |
| 8 | Weight (kg) | 1.9 | 2 | 0.5 |
| 9 | Dimensions (mm) | 645x285x18 | 645x285x18 | 645x285x18 |

To evaluate the effect of dust deposition on the output power of PV modules, a Photovoltaic Solar Energy Modular Trainer (EDQUIP) at Al Furat Al Awsat Technical University (FATU) was used. The set-up consists of; ED-9710-4 Central Communication Module, ED-9710-3 Energy Storage Module, ED-9710-2 DC/AC Inverter Module, Sun Simulation Module (variable light intensity bulb), DC Voltage meter, DC Current meter, Modified Sinewave AC Voltage meter, Modified Sinewave AC Current meter, and Solar Panel horizontal mounting deck. For the purpose of digital data logger, an interface through ARDUINO Card with 16 MHZ processor was implemented. The card consists of; 2KB SRAM& 32KB FLASH memory, 14 digital I/O, and 6 analog I/O, Voltage Sensor, and Current Sensor. The set-up is shown in Figure1.

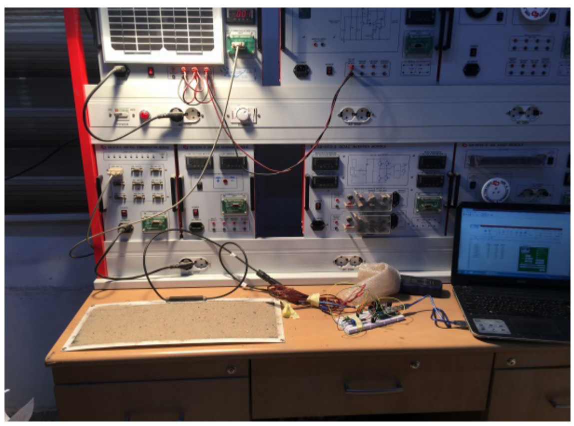

FIGURE 1. Photographic Image of the set-up

The three modules (monocrystalline, polycrystalline, and thin-film PV modules) were horizontally and sequentially mounted directly 100 cm under a fixed load solar radiation simulator of 1000 watt/m2. For each module; measurements of voltage and current for clean and dust-deposited surface were conducted. For dust-deposited surfaces; 0, 12, and 24 gm were dispersed to build different thickness layers on the surface of each type of modules. The efficiency of each module and the percent of its power drop were calculated using equations (7) and (8).

$$\eta = \frac{P_{deposit}}{P_{clean}} x100 \quad (7)$$

$$\% P_{drop} = \frac{P_{clean} - P_{deposit}}{P_{clean}} x100 \quad (8)$$

Where; η: PV module efficiency, $P_{clean}$: Output powerfor clean surface module, $P_{deposit}$: Output power for dust-deposited surface module, $P_{drop}$: Output power drop due to dust.

## RESULTS AND DISCUSSIONS

### DUST DISPERSION AND DEPOSITION

Downwind (Axial) dust concentration (mg/m3) due to dispersion phenomenon at different wind velocities (1, 3, 5, 7, and 9 m/s) were calculated using Gaussian-Plume model and presented in Figure 2. It is clearly seen that dust concentration spatially increases from point source up to a distance of 1-3 km, then it sharply declines to minimum concentration beyond 10 km. The higher the wind velocity is the lower the dust concentration. This may be attributed to non-stable atmosphere at velocities higher than 6 m/s which may cause high lateral (crosswind) dispersion. However, the prevailing wind velocity at the regions where this study was conducted is 3-4 m/s. The prevailing wind velocity lays at the stable atmosphere conditions leading to relatively dominant axial dispersion of industrial dust particles.

## SPECTROPHOTOMETRIC AND CRYSTALLOGRAPHY STUDIES

### GRAPHENE

Graphene is simply an allotrope Carbon. It was selected for this study as a representative of industrial pollutants. Carbon and carbon compounds represent common pollutant that disperse in the atmosphere as fine particulates. Figure (3) shows the spectral characteristics of Graphene.

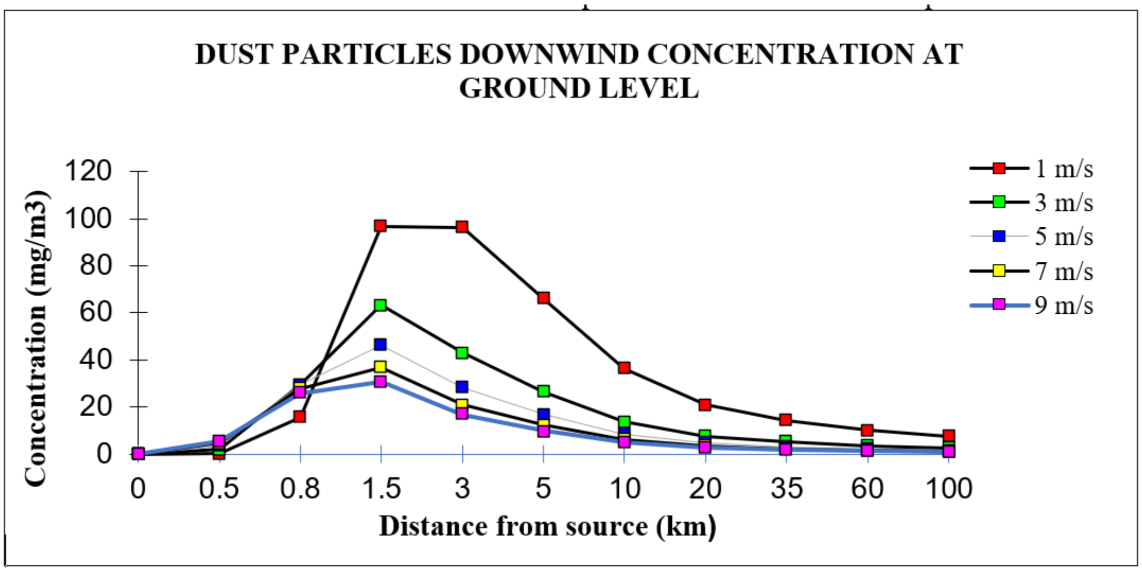


FIGURE 2. Downwind (axial) dust particles spatial concentration profile (mg/m3) at different wind velocities.

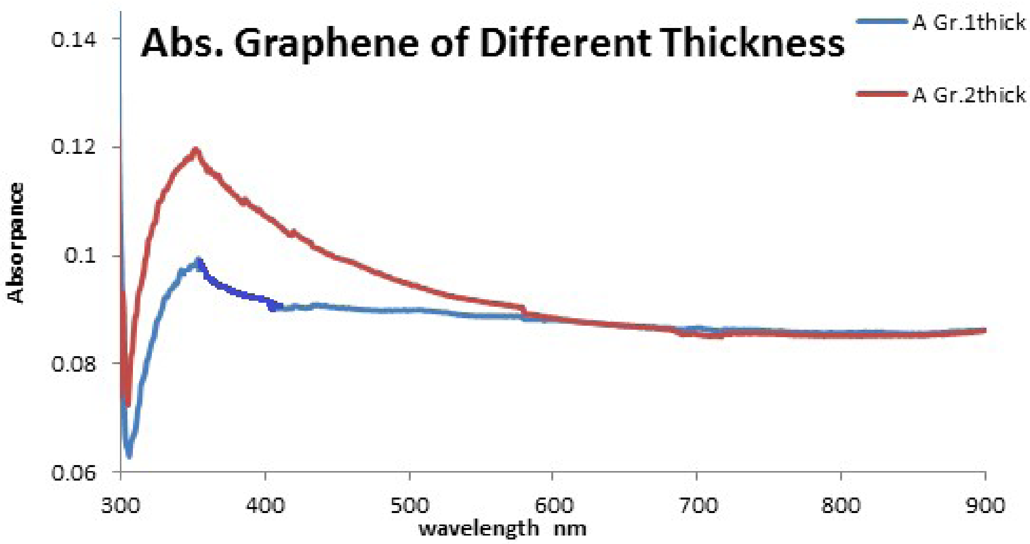
Abs. Graphene of Different Thickness
A Gr.1thick
A Gr.2thick
Absorpance
0.14
0.12
0.1
0.08
0.06
300
400
500
600
700
800
900
wavelength nm

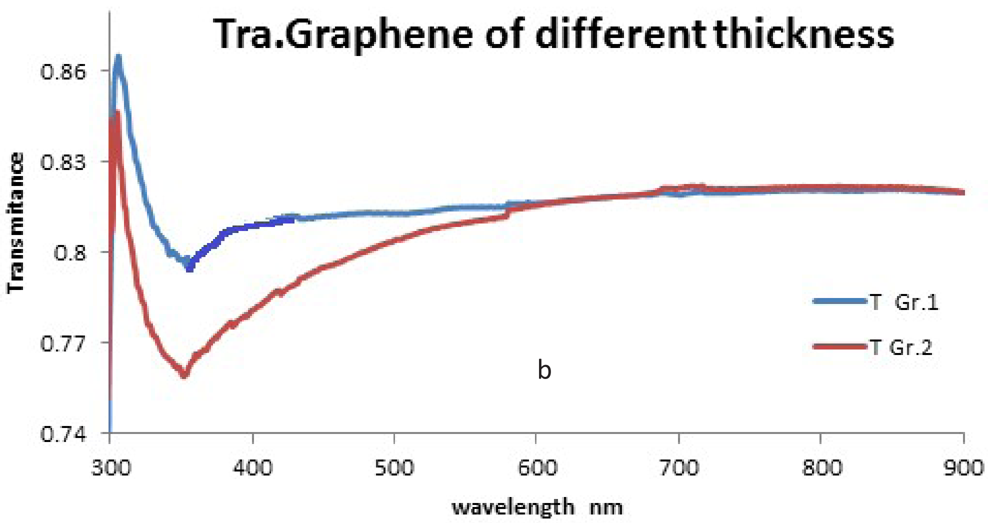
Tra.Graphene of different thickness
Transmitance
0.86
0.83
0.8
0.77
0.74
T Gr.1
T Gr.2
b
300
400
500
600
700
800
900
wavelength nm

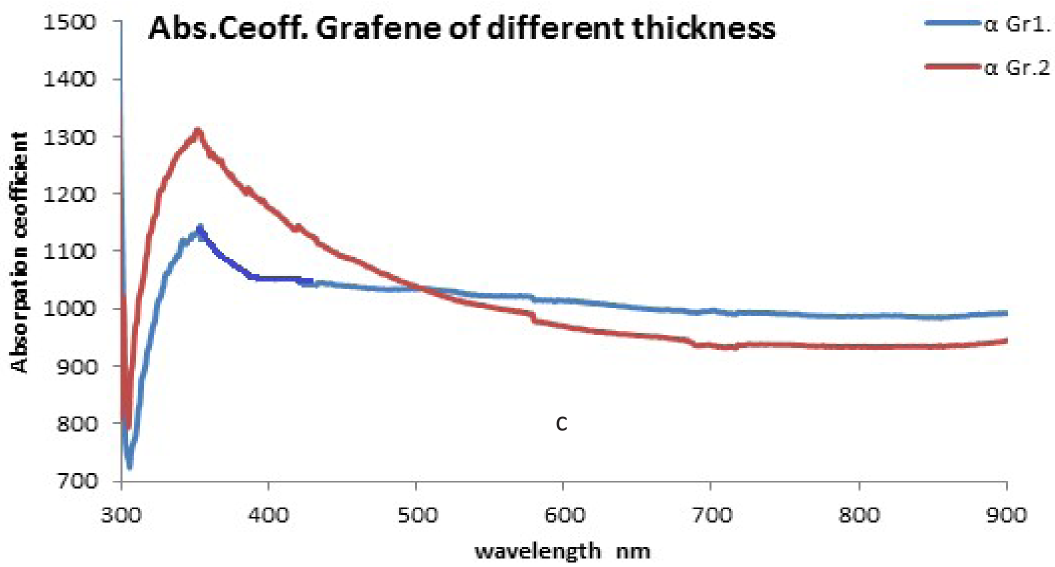
Abs.Ceoff. Grafene of different thickness
α Gr1.
α Gr.2
Absorpation ceofficient
1500
1400
1300
1200
1100
1000
900
800
700
c
300
400
500
600
700
800
900
wavelength nm

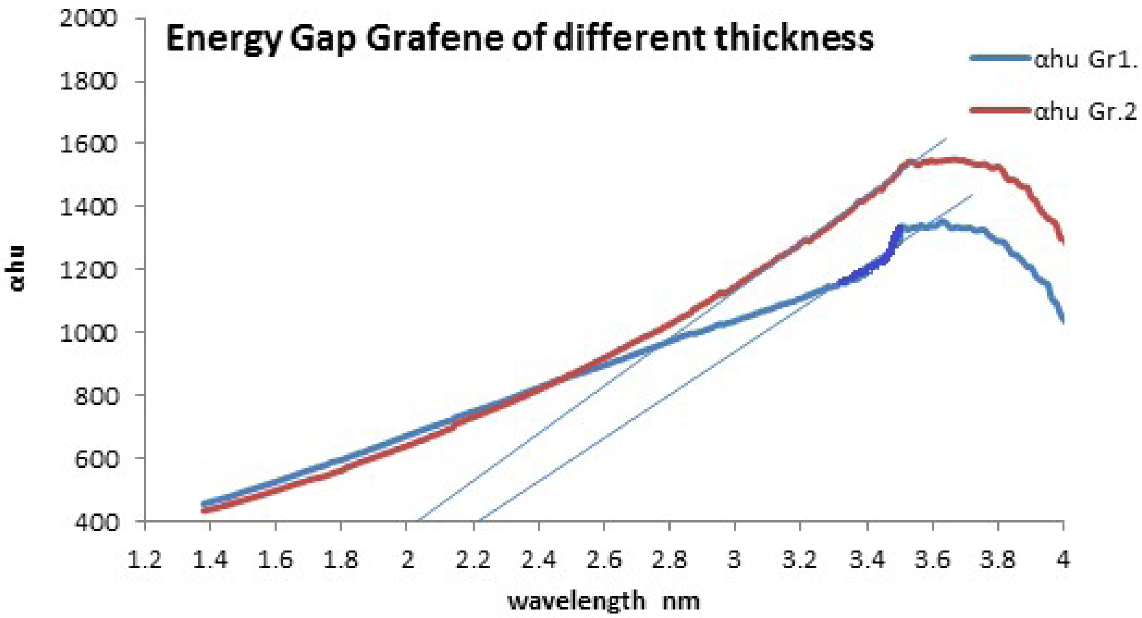


FIGURE 2. Spectral characteristics of Graphene; A: Absorbance, B: Transmittance ,C: Absorbance coefficient, D: Energy gap.

Figure 3-a demonstrates that the absorbance spectra of Graphene is located within the UV spectrum (350 nm). It is clearly shown that the Graphene absorbance at the UV spectrum depends on its layer thickness (length of light path) following Beer Lambert law. The higher the thickness of Graphene layer is the higher UV spectrum absorption. At the visible spectrum, the Graphene absorbance becomes independent of its layer thickness. Figure 3-b shows that the transmittance spectra of Graphene is also located within the UV spectrum and shows minimum transmittance. Figure 3-c shows that the absorbance coefficient of Graphene reflects the trend of Graphene to be excited when absorb light and an atomic electron transition (jump) takes place. This means that the absorbed energy of incident light promotes Graphene to an excited state. Figure 3-d explains the energy gap of Graphene. Energy gap is the difference of energy between the bottom of the conduction band and the top of the valence band of the electrons in a crystalline. It is clearly seen that the energy gap is located within the semiconductor range (0.9-3.5 ev). Therefore, Graphene has high negative impact on PV cells due to its spectrophotometric characteristics.

Figure 4 demonstrates XRD and SEM images of Graphene powder. XRD image (Fig. 4-a) indicate that Graphene sample is pure and has crystalline structure, as it shows a unique spike at 2-theta of 27. Crystalline materials usually reflect part of the incident light. Therefore, it is expected to negatively contribute in obscuring incident light and reducing its transmittance through the Graphene layer.

The SEM image of Graphene (Fig. 4-b) shows that Graphene agglomerates under wet conditions. Agglomeration negatively affect light transmittance as particles become condensed and reduce spaces and voids of the deposited layer.

## SILICA

Figure 5-a shows that Silica has no absorbance of light. Low absorbance materials are classified as insulators. Insulators have large energy gap and effectively resist electron transition (jump). Therefore, the only effect of Silica deposited layers were their resistance to light transmittance. The resistance was found to be layer thickness dependent. Figure 5-b shows Silica transmittance and clearly indicates that the percent of transmitted light depends on the deposited layer thickness.

Figure 6 shows XRD and SEM images of Silica. Silica has an amorphous structure as it exhibits a broad spectrum (Fig. 6-a). Amorphous materials have low light reflection and exhibits only light obscuring characteristic. Their resistance to light transmittance depends on the thickness of the deposited layer. SEM image of Silica (Fig. 6-b) suggests a hilly structure of Silica powder. Silica ranges from spherical to fiber shapes with dimensions range from 1 to 3 µm. Multilayers of Silica powder were noticed

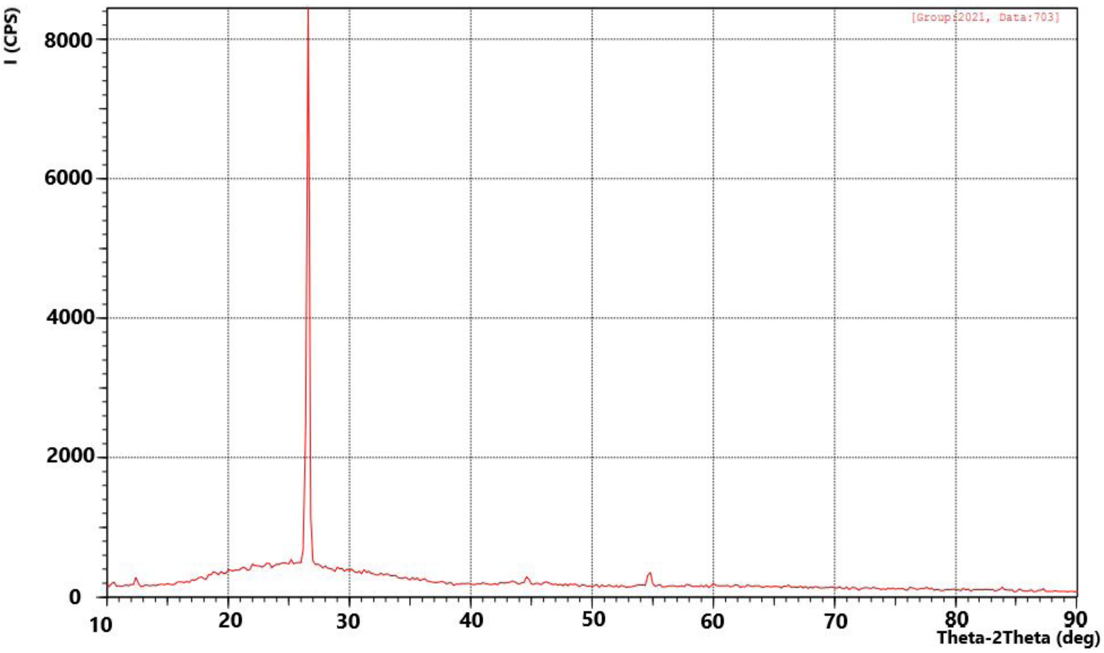


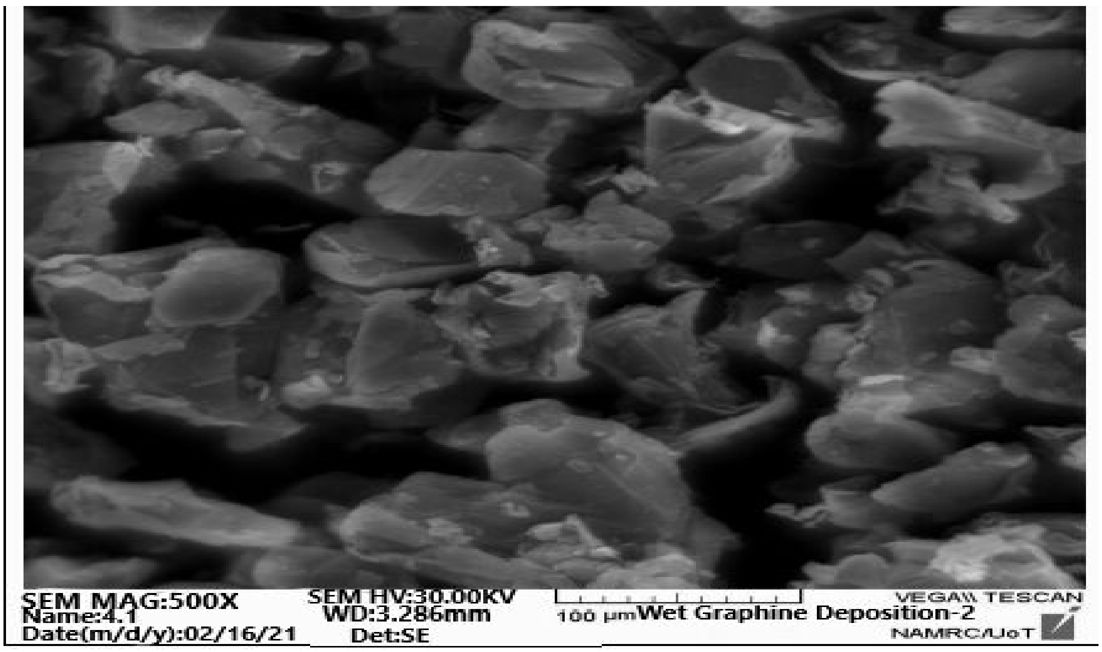


FIGURE 4. XRD and SEM images of Graphene; a: XRD, b: SEM

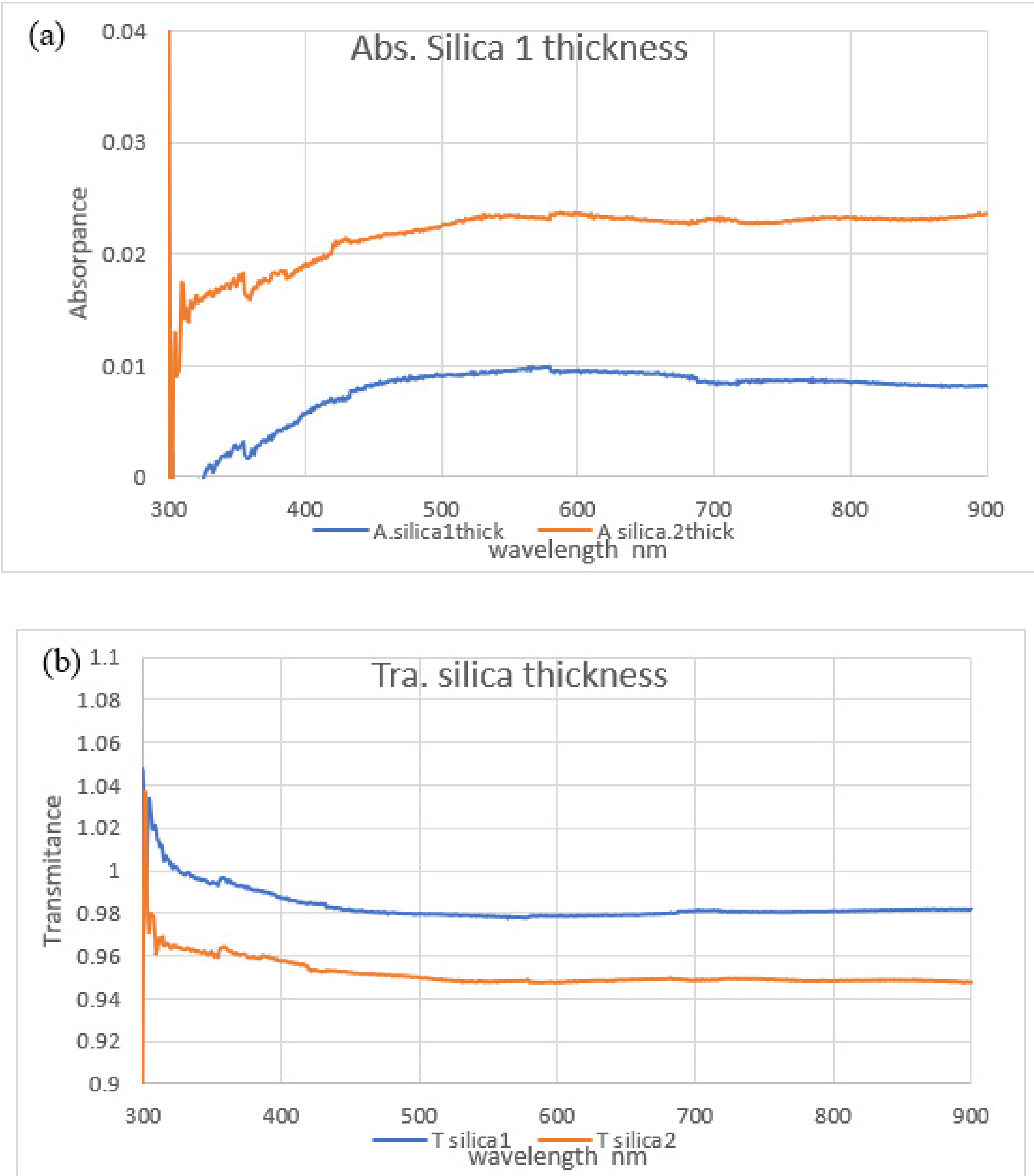


FIGURE 5. Spectral Characteristics of Silica; (a) Absorbance, (b) Transmittance

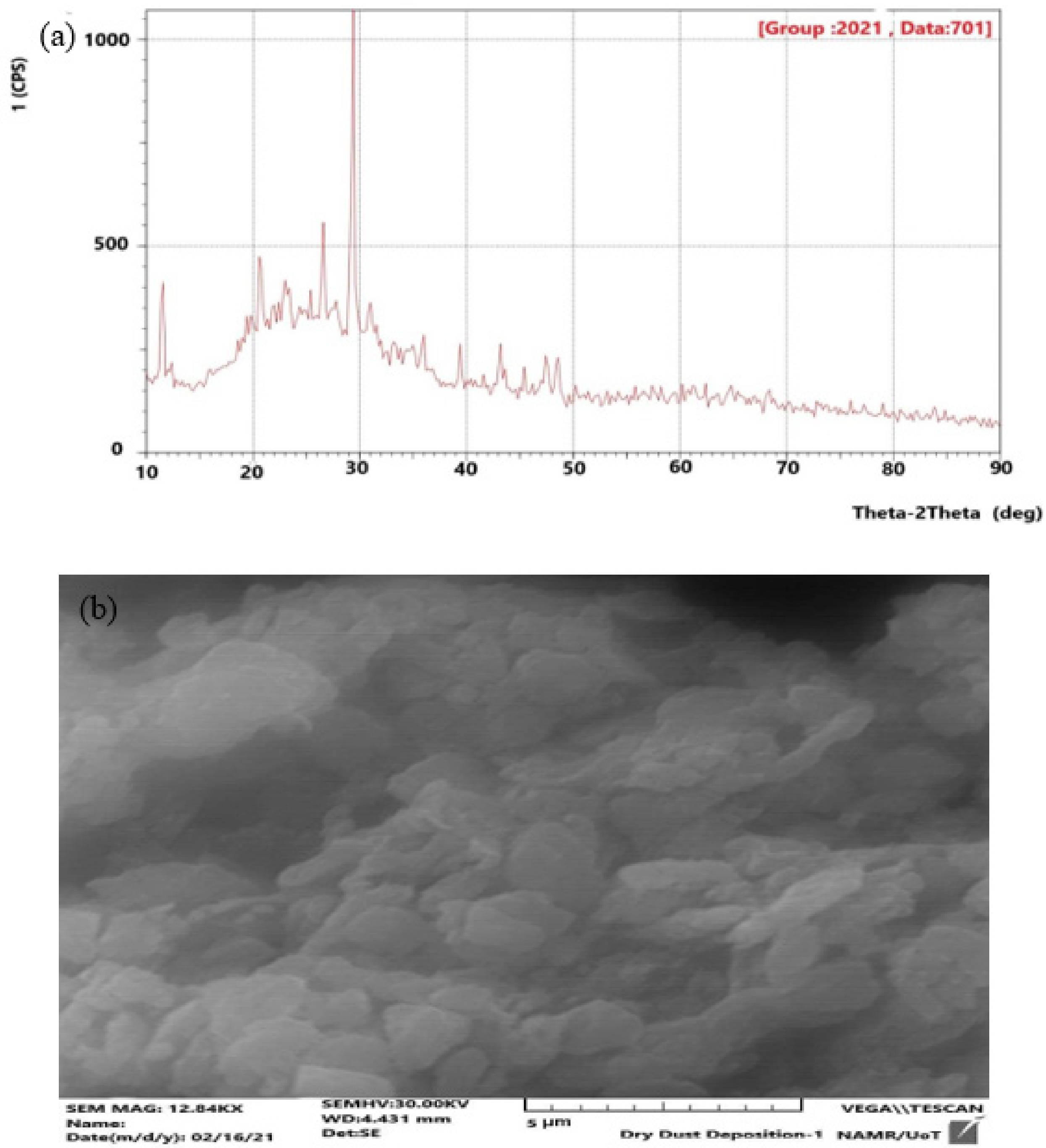


FIGURE 6. XRD and SEM images of Silica, (a) XRD, (b) SEM

NATURAL DUST

Natural dust in Iraq is composed of silicate and carbonate. Calcite is the main mineral in most of Iraq. Therefore, the chemical composition of the natural dust in Iraq is mainly Silicon compounds. It was confirmed through the spectral and crystallography tests of Silicon and natural dust. They were similar and little differences were observed. Figure 7 demonstrates optical absorbance and transmittance of natural dust. Natural dust has no absorbance and its transmittance depends on the deposited layer thickness. This indicates that natural dust is an optical insulator material due to its wide energy gap. Figures 7-a and 7-b show the absorbance and transmittance of natural dust respectively.

Figure 8 shows XRD and SEM images of natural dust. Natural dust has an amorphous structure as XRD test shows broad spectrum (Fig. 8-a). Narrow spikes were observed in the XRD spectra indicating that natural dust was mixture of many minerals. Its impact on light transmittance is layer thickness dependent. SEM image of natural dust (Fig. 8-b) shows that natural dust agglomerates as blocks to create voids and spaces between agglomerated blocks. The spaces and voids allow light transmittance to suggest that natural dust has least effect in comparison with Graphene and Silica.

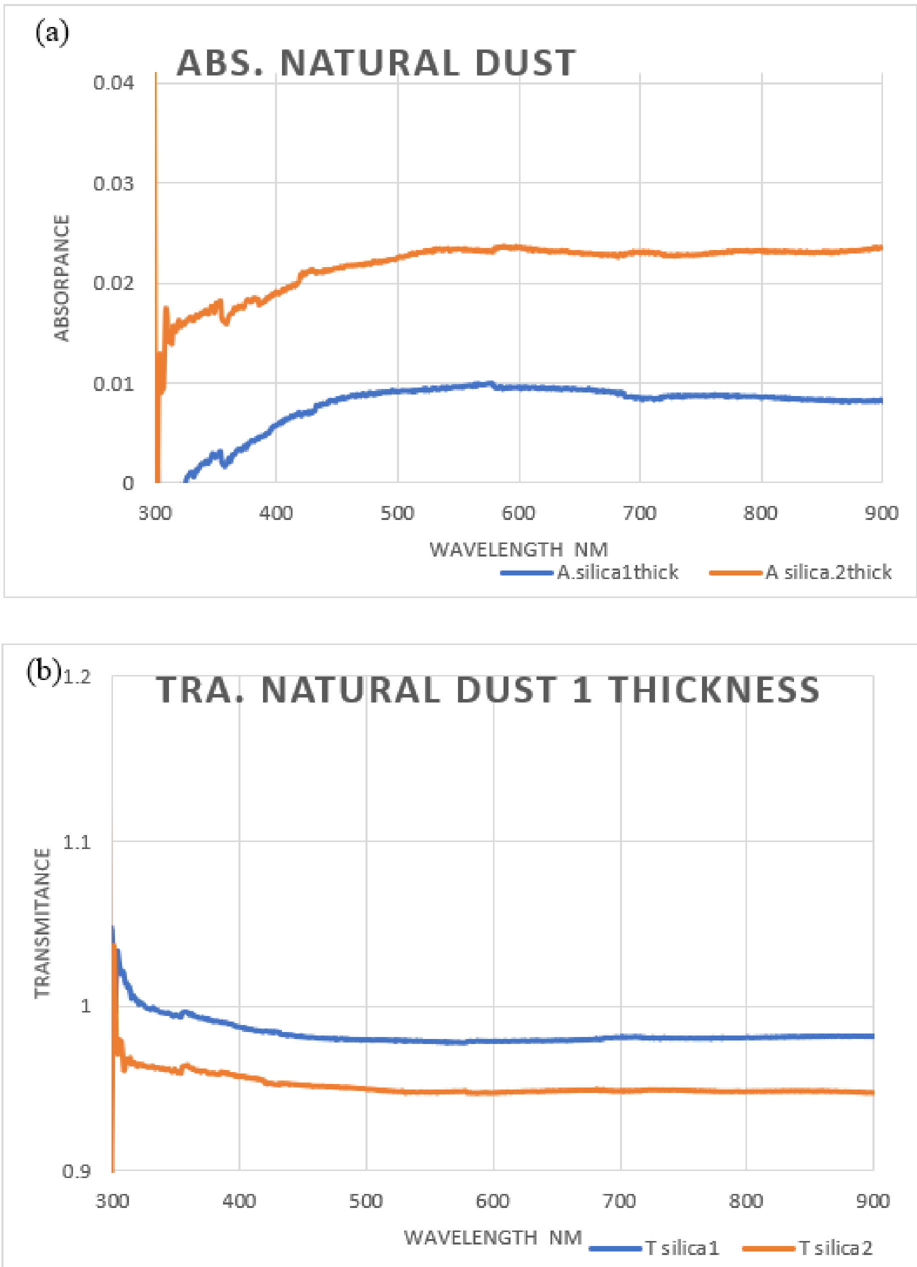


FIGURE 7. Spectral characteristics of natural dust; (a) Absorbance, (b) Transmittance

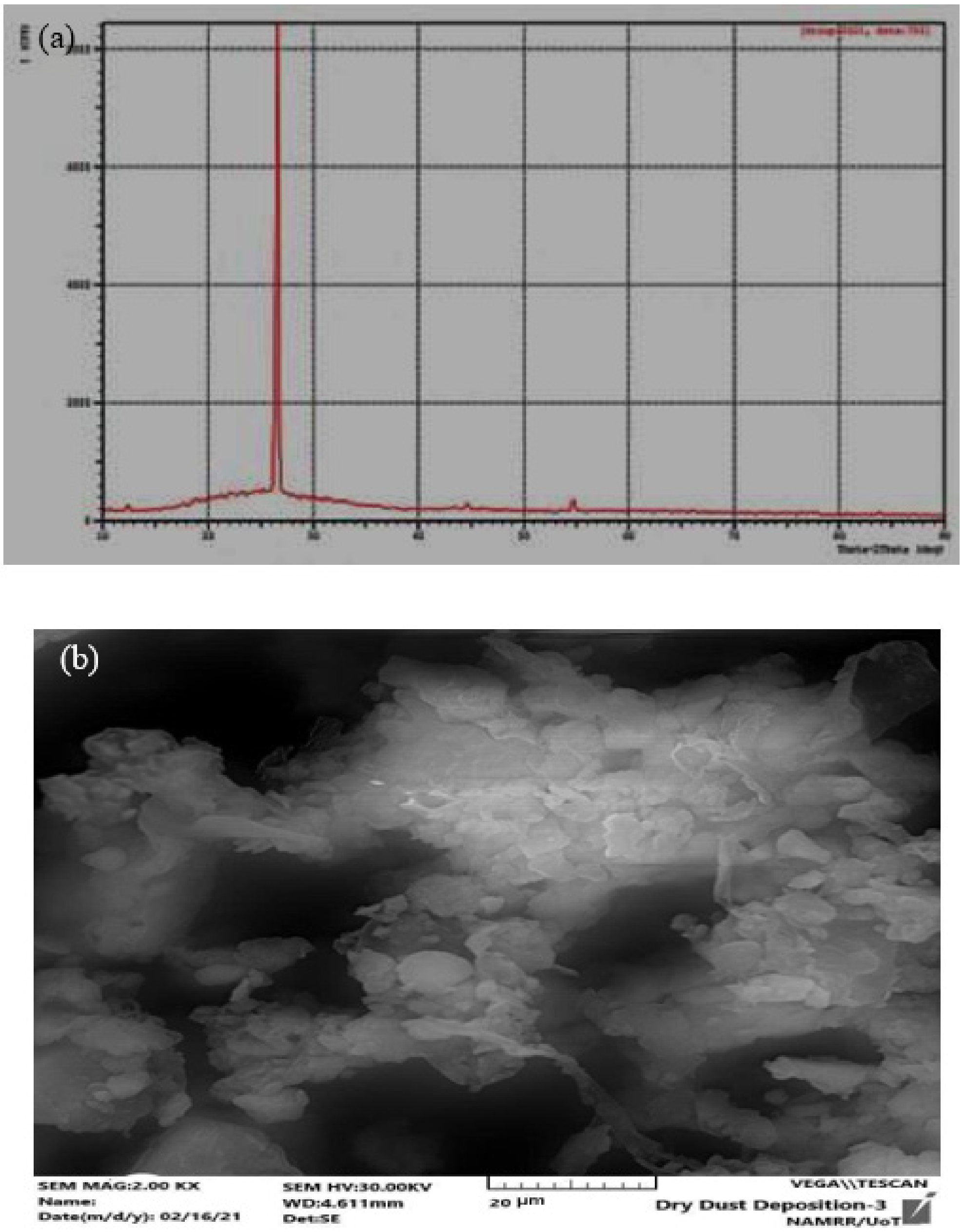


FIGURE 8. XRD and SEM images of natural dust; a: XRD, b: SEM

## PV PERFORMANCE

Tables 1, 2, and 3 summarize the degradation rates of the output powers of monocrystalline, polycrystalline, and thin-film PV modules as a function of different layer thickness of Graphene, Silica, and natural dust. The results demonstrate the PV efficiency and the percentage of power drop for monocrystalline, polycrystalline, and thin-film PV modules under different thicknesses of Graphene, Silica, and Natural dusts. Graphene dust exerted major effect on the performance of the PV modules. It exerted 70%, 71%, 96% output power reduction for monocrystalline, polycrystalline, and thin-film PV modules respectively. High output power drop of thin-film PV module was expected as the Graphene dust directly deposited on PV cells. Silica and natural dust exerted lower impacts on the three types of PV modules.

Silica and natural dust exhibited in similar manner because of their close chemical composition. XRD tests showed that Silica sample was free of impurities, while the natural dust sample was a mixture of Silicon compounds.The results of PV performance measurements agree with the interpretations of the spectrophotometric and crystallographic investigations. As shown previously, Graphene has major impact on light transmittance due to its light absorbance property. Silica and natural dust showed lower output power drop because of their amorphous structure. The obtained results confirm that the large difference of impact of the three types of dust is related to dust spectral characteristics. This agrees with Chanchangi et al. (2020) findings.

The large drop in the performance of the thin-film PV module due to Graphene may be attributed to the electrostatic forces which promote inter-particle adhesion [Chanchangi et al. 2020]. The amorphous structure of Silica and natural dust resulted in lower deterioration of the performance of the three types of PV modules. It was observed that their effects depend on the deposited layer thickness. This agrees with Husain et al. (2020) conclusions and observations

TABLE 2. Graphene, Silica, and Natural dust effect on the performance of the monocrystalline PV module

| No | Dust type | Monocrystalline PV module | | | | | | | |
|---|---|---|---|---|---|---|---|---|---|
| | | Mass (gm) | Layer Thick (μm) | VOC (V) | ISC (A) | $P_{max}$ (w) | Rad. (w/m$^2$) | η% output power | % drop power |
| 1 | Graphene | 0 | 0 | 17.83 | 1.25 | 22.28 | 1000 | 100 | 0 |
| | | 12 | 0.237 | 10.26 | 1.24 | 12.72 | 1000 | 57 | 43 |
| | | 24 | 0.574 | 5.34 | 1.24 | 6.62 | 1000 | 30 | 70 |
| 2 | Silica | 0 | 0 | 17.83 | 1.25 | 22.28 | 1000 | 100 | 0 |
| | | 12 | 0.4 | 16.98 | 1.24 | 21.05 | 1000 | 94 | 6 |
| | | 24 | 0.8 | 15.5 | 1.24 | 19.22 | 1000 | 86 | 14 |
| 3 | Natural dust | 0 | 0 | 17.83 | 1.25 | 22.28 | 1000 | 100 | 0 |
| | | 12 | 0.438 | 15.4 | 1.24 | 19.09 | 1000 | 85.6 | 14.4 |
| | | 24 | 0.876 | 14.21 | 1.24 | 17.62 | 1000 | 79 | 21 |

TABLE 3. Graphene, Silica, and Natural dust effect on the performance of the polycrystalline PV module

| No | Dust type | Monocrystalline PV module | | | | | | | |
|---|---|---|---|---|---|---|---|---|---|
| | | Mass (gm) | Layer Thick (μm) | VOC (V) | ISC (A) | $P_{max}$ (w) | Rad. (w/m$^2$) | η% output power | %drop power |
| 1 | Graphene | 0 | 0 | 17.68 | 1.25 | 22.1 | 1000 | 100 | 0 |
| | | 12 | 0.237 | 10.16 | 1.24 | 12.6 | 1000 | 57 | 43 |
| | | 24 | 0.574 | 5.14 | 1.24 | 6.4 | 1000 | 29 | 71 |
| 2 | Silica | 0 | 0 | 17.68 | 1.25 | 22.1 | 1000 | 100 | 0 |
| | | 12 | 0.4 | 14.9 | 1.24 | 21.08 | 1000 | 91 | 16.4 |
| | | 24 | 0.8 | 14.02 | 1.24 | 18.12 | 1000 | 82 | 21 |
| 3 | Natural dust | 0 | 0 | 17.68 | 1.25 | 22.1 | 1000 | 100 | 0 |
| | | 12 | 0.438 | 16.2 | 1.24 | 18.47 | 1000 | 83 | 9.1 |
| | | 0 | 0 | 17.68 | 1.25 | 22.1 | 1000 | 100 | 0 |

TABLE 4. Graphene, Silica, and Natural dust effect on the performance of the thin-film PV module

| No | | Monocrystalline PV module | | | | | | | |
|---|---|---|---|---|---|---|---|---|---|
| | | Mass (gm) | Layer Thick (μm) | VOC (V) | ISC (A) | $P_{max}$ (w) | Rad. (w/m$^2$) | η% output power | %drop power |
| 1 | Graphene | 0 | 0 | 15.1 | 1.25 | 20.3 | 1000 | 100 | 0 |
| | | 12 | 0.47 | 4.6 | 1.24 | 5.05 | 1000 | 24.8 | 75.1 |
| | | 24 | 0.94 | 0.6 | 1.24 | 0.744 | 1000 | 3.94 | 96 |
| 2 | Silica | 0 | 0 | 16.24 | 1.25 | 20.3 | 1000 | 100 | 0 |
| | | 12 | 0.65 | 15.75 | 1.24 | 19.53 | 1000 | 96.2 | 3.79 |
| | | 24 | 1.3 | 12.3 | 1.24 | 15.26 | 1000 | 75.1 | 24.8 |
| 3 | Natural dust | 0 | 0 | 16.24 | 1.25 | 20.3 | 1000 | 100 | 0 |
| | | 12 | 0.71 | 14.58 | 1.24 | 18.09 | 1000 | 89.1 | 10.8 |
| | | 24 | 1.42 | 11.98 | 1.24 | 14.68 | 1000 | 73.2 | 26.79 |

## CONCLUSION

The effect of three types of dust (Graphene, Silica, and natural dust) on three types of PV modules was investigated. Spectral characteristics of dust were found to impact the performance of PV modules. It was found that semi conductive materials exhibit considerable light absorbance within the UV spectrum, while optically insulators materials showed insignificant light absorption. Therefore, identifying optically conductive dusts is of importance for the site selection process of solar farms. The most dominant industrial particles dispersed in urban areas is carbon and carbon derivatives such as graphite, ash, graphene, ...etc. Therefore, extensive investigations are necessary to map the air pollution of proposed areas for solar systems installations. The crystallography studies of dust were proved important for solar system design as the degradation of PV modules proved to be layer thickness dependent for amorphous structure dusts. Also, evaluating the tilt angle of a solar panel against gravity sliding of particles is necessary.

## ACKNOWLEDGEMENT

This research work was supported by the Ministry of Higher Education Malaysia under the Fundamental Research Grant Scheme (FRGS/1/2020/TK0/UKM/02/11) and Universiti Kebangsaan Malaysia Grant under Geran Universiti Penyelidikan (GUP-2022-024).

## DECLARATION OF COMPETING INTEREST

None

## REFERENCES

Chanchangi, Y.N., Ghosh, A., Sundaram, S., Mallik, T.K., 2020. An analytical indoor experimental study on the effect of soiling on PV, focusing on dust properties and PV surface material. *Sol. Energy* 203: 46-68.

Costa, S.C.S, Diniz, A.S.A.C., Kazmerski, L.L., 2018. Solar energy dust and soiling R&D progress: literature review update for 2016. Rnew. Sustain. *Energy Rev.* 82 (3): 2504-2536.

Hussain, A., Batra, A., Pachauri, R., 2017. An experimental study on the effect of dust on power loss in solar photovoltaic module. Renewables; Wind, Water, and Solar 4:9.

Darwish, Z. A. (2013). Impact of some environmental variables with dust on solar photovoltaic: Review and research. *International Journal of Energy and Environment*, 7(4): 152–159.

Negash, T., Tadiwose, T., 2015. Experimental investigation of the effect of tilt angle on the dust photovoltaic module. *Int. J. Energy Power Eng.* 4 (4): 227–231.

Gandhi, T., Gupta, A., Shyam, B. 2014. Investigation of the effects of dust accumulation, and performance for mono and poly-crystalline silica modules. *Int. J. Renew. Energy Res.* 4(3).

Darwish, Z., Kazem, H., Sopian, K., Al-Goul, M., Alawadhi, H. 2015. Effect of dust pollutant type on photovoltaic performance. *Renew. Sust. Energy Rev.* 41: 735–744.

Zang, J., Wang, Y. 2011. Analysis of computation model of particle deposition on transmittance for photovoltaic panels. *Energy Proc.* 12: 554–559.

Hussein A Kazem1, Miqdam T Chaichan. 2016. Effect of Environmental Variables on Photovoltaic Performance-Based on Experimental Studies. *International Journal of Civil, Mechanical and Energy Science (IJCMES)* 2(4).

M. T. Chaichan, B. A. Mohammedand H. A. Kazem. 2015. Effect of pollution and cleaning on photovoltaic performance based on experimental study. *International Journal of Scientific and Engineering Research* 6(4): 594-601.

Z. A. Darwish, H. A. Kazem, K. Sopian, M. A. Alghoul and M. T. Chaichan. 2013. Impact of some environmental variables with dust on solar photovoltaic (PV) performance: review and research status. *International J of Energy and Environment* 7(4): 152-159.

Hegazy, A., 2001. Effect of dust accumulation on solar transmittance through glass covers of plate-type collectors. *Renew. Energy* 22(4): 525–540.

Fountoukis, C., Figgis, B., Ackermann, L., Ayoub, M.A. 2018. Effects of atmospheric dust deposition on solar PV energy production in a desert environment. *Sol. Energy* 164: 94-100.

El-Shobokshy, M.S., Hussein, F.M. 1993a. Degradation of photovoltaic cell performance due to dust deposition on to its surface. *Renew. Energy* 3 (6-7): 585-590.

Kazem, H.A., Chaichan, M.T. 2019. The effect of dust accumulation and cleaning methods on PV panels' outcomes based on an experimental study of six locations in Northern Oman. *Sol. Energy* 187: 30-K38.

Chaichan, M.T., Kazem, H.A., Al-Waeli, A.H., Sopian, K. 2020. The effect of dust components and contaminants on the performance of photovoltaic for the four regions in Iraq: A practical study. *Renewable Energy and Environmental Sustainability* 5: 3.

Chen, J., Pan, G., Ouyang, J., Ma, J., Fu, L., Zhang, L., 2020. Study on impacts of dust accumulation and rainfall on PV power reduction in East China. *Energy*, 116915.

Styszko, K., Samek, L., Szramowiat, K., Korzeniewska, A., Kubisty, K., Rakoczy-Lelek, R., Kistler, M. & Giebl, A. K. 2017. Oxidative potential of PM10 and PM2. 5 collected at high air pollution site related to chemical composition: Krakow case study. *Air*

*Qual Atmos Health* 10:1123–1137. https://doi.org/10.1007/s11869-017-0499-3

Fujiwara, F., Rebagliati, R. J., Dawidowski, L., Gómez, D., Polla, G., Pereyra, V. & Smichowski, P. 2011. Spatial and chemical patterns of size fractionated road dust collected in a megacitiy. *Atmos Environ* 45:1497–1505. https://doi.org/10.1016/j.atmosenv.2010.12.053

Bi, X., Liang, S. & Li, X. 2013. A novel in situ method for sampling urban soil dust: Particle size distribution, trace metal concentrations, and stable lead isotopes. *Environ Pollut* 177: 48–57. https://doi.org/10.1016/j.envpol.2013.01.045

Sarver, T., Al-Qaraghuli, A. & Kazmerski, L. L. 2013. A comprehensive review of the impact of dust on the use of solar energy: history, investigations, results, literature, and mitigation approaches. *Renew Sust Energ Rev* 22: 698–733. https://doi.org/10.1016/j.rser.2012.12.065.

Hassan, Q., Jaszczur, M. & Przenzak, E. 2017. Mathematical model for the power generation from arbitrarily oriented photovoltaic panel. *E3S Web of Conferences* 14:01028. https://doi.org/10.1051/e3sconf/20171401028.

Benatiallah A, Ali AM, Abidi F, Benatiallah D, Harrouz A, Mansouri I (2012) Experimental study of dust effect in mult-crystal PV solar module. *Int J Multidisciplinary Sci Eng* 3:1–4.

Pang H, Close J, Lam K H, (2006) Study on effect of urban pollution to performance of commercial copper indium diselenide modules, 2:2195–2198. https://doi.org/10.1109/WCPEC.2006.279943.

Hinds WC (1999) *Aerosol technology: properties, behavior, and measurement of airborne particles*. John Wiley & Sons, Hoboken.

Ndiaye A, Kébé CM, Ndiaye PA, Charki A, Kobi A, Sambou V (2013) Impact of dust on the photovoltaic (PV)modules characteristics after an exposition year in Sahelian environment: the case of Senegal. *Int J Phys Sci* 8:1166–1173. https://doi.org/10.5897/IJPS2013.3921.

Bashir MA, Ali HM, Ali M, Siddiqui AM (2015) An experimental investigation of performance of photovoltaic modules in Pakistan. *Therm Sci* 19:525–534.

Ali HM, Mahmood M, BashirMA, Ali M, Siddiqui AM (2016) Outdoor testing of photovoltaic modules during summer in Taxila, Pakistan. *Therm Sci* 20:165–173.

Darwish, A.D., Sopian, K., Fudholi, A. (2021). Reduced output of photovoltaic modules due to different types of dust particles. *Journal of cleaner production* 280 (2021) 124317.

Macdonald, R., THEORY AND OBJECTIVES OF AIR DISPERSION MODELLING, MME 474A Wind Engineering, 2003.

Li Yang and Irina Harun, Renewable Energy scenarios for sustainable Electricity in Malaysia and the Application of Analytical Hierarchy process (AHP) for Decision making, *Jurnal Kejuruteraan* 34(6) 2022: 1271-1279.

Das, H. S., Salem, M., Zainuri, M. A. A. M., Dobi, A. M., Li, S., & Ullah, M. H. (2022). A comprehensive review on power conditioning units and control techniques in fuel cell hybrid systems. *Energy Reports*, 8, 14236-14258.

Hamidi, M. N., Ishak, D., Zainuri, M. A. A. M., Ooi, C. A., & Tarmizi, T. (2020). Asymmetrical multi-level dc-link inverter for pv energy system with perturb and observe based voltage regulator and capacitor compensator. *Journal of Modern Power Systems and Clean Energy* 9(1): 199-209.

Khawaja, A. W., Kamari, N. A. M., & Zainuri, M. A. A. M. 2021. Design of a damping controller using the SCA optimization technique for the improvement of small signal stability of a single machine connected to an infinite bus system. *Energies* 14(11): 2996.

Hamidi, M. N., Ishak, D., Zainuri, M. A. A. M. & Ooi, C. A. 2020. An asymmetrical multilevel inverter with optimum number of components based on new basic structure for photovoltaic renewable energy system. *Solar Energy* 204: 13-25.

Charin, C., Ishak, D., Mohd Zainuri, M. A. A., & Ismail, B. 2021. Modified levy flight optimization for a maximum power point tracking algorithm under partial shading. *Applied Sciences* 11(3): 992.

Abutaima, K. A. & Mohamed, R. 2022. Design of improved incremental conductance with Fast Intelligent (FI) based MPPT Technique for solar PV system. *Jurnal Kejuruteraan* 34(6): 1093-1104.